Talanta 200 (2019) 480–486

Contents lists available at ScienceDirect

Talanta

journal homepage: www.elsevier.com/locate/talanta

# Label-free fluorescence detection of circulating microRNAs based on duplex-specific nuclease-assisted target recycling coupled with rolling circle amplification

Tingting Fan[a,b], Yu Mao[c,*], Feng Liu[b], Wei Zhang[b], Jin-Shun Lin[b], Jingxian Yin[a,b], Ying Tan[b], Xiaoting Huang[a,b], Yuyang Jiang[a,b,**]

[a] Department of Chemistry, Tsinghua University, Beijing 100084, PR China
[b] State Key Laboratory of Chemical Oncogenomics, Key Laboratory of Chemical Biology, the Graduate School at Shenzhen, Tsinghua University, Shenzhen 518055, PR China
[c] School of Food and Biological Engineering, Hefei University of Technology, Hefei 230009, PR China

ARTICLE INFO

*Keywords:*
Serum circulating microRNAs
Duplex specific nuclease
Rolling circle amplification
Biosensor
SYBR gold dye

ABSTRACT

A simpler, more rapid and selective biosensor has been developed for the sensitive detection of circulating miRNAs (c-miRNAs) based on duplex-specific nuclease (DSN)-assisted target recycling coupled with rolling circle amplification (RCA) using SYBR Gold Dye as a signal indicator. This biosensor exhibits a tremendously low detection limit of 0.3 fM of c-miRNAs and shows high selectivity for one-base mismatched c-miRNA. In addition, most importantly, the biosensor could accurately determine the amounts of target c-miRNA in total c-miRNAs isolated from human serums and human cancer cell lines, which confirms that the biosensor could be used to quantify c-miRNAs in complex biological samples and for the clinical early diagnosis of cancers based on c-miRNAs detection.

## 1. Introduction

Circulating microRNAs (c-miRNAs) are endogenous noncoding small RNAs (approximately 18–24 nt) that circulate in body fluids, including plasma [1], serum [2], urine [3], saliva [4], and semen [5]. They can regulate target gene expression by degrading mRNAs or repressing the translation of mRNAs [6,7] and thus guide many biological processes, such as cell proliferation, cell differentiation, cell apoptosis and the occurrence of several diseases, especially cancers [8–10]. Moreover, some c-miRNAs have been successfully demonstrated as biomarkers for cardiovascular disease [11], acute stroke [12], and several cancers, such as breast cancer [13], lung cancer [2], urologic cancer [14], *etc*. Therefore, much effort has been devoted over the past decades to the development of c-miRNAs detection, such as via northern blotting [15], microarrays [16], and quantitative real-time PCR (qRT-PCR) [17]. Despite their remarkable advantages, these systems suffer from certain limitations, including lower sensitivity, higher false-positive rates, and multistep reactions from the viewpoint of their practical application. Consequently, it is highly demanding to develop much simpler, more sensitive and selective protocols for the rapid detection of c-miRNAs in biological assays. Remarkable progress on the c-miRNAs assay has been witnessed in recent years, such as electrochemical sensing [18,19], chemiluminescence [20,21], isothermal nucleic acid amplification [22,23], and nanoparticle sensing [24,25]. Among these impressive approaches, rolling circle amplification (RCA), a constant temperature amplification strategy, has attracted much attention for c-miRNAs assay because of its higher sensitivity, better specificity, and simplicity [26–28]. RCA is an advanced isothermal enzymatic process (acting at room temperature to 37 °C) [29] that uses unique DNA or RNA polymerases (phi29 DNA polymerase, Klenow Fragment (3'– > 5' exo-), and T7 RNA polymerase) to produce long, single-stranded DNA or RNA (ssDNA, ssRNA) [30,31] by continuously adding nucleotides (nt) to a primer complementary to a circular template, resulting in a long ssDNA with thousands of tandem repeat sequences.

Duplex-specific nuclease (DSN) is a commercial, heat-resistant nuclease [32] that is considered to be a promising tool for biology analysis due to its distinctive capability to cleave only double-stranded DNA

* Corresponding author.
** Corresponding author at: State Key Laboratory of Chemical Oncogenomics, Key Laboratory of Chemical Biology, the Graduate School at Shenzhen, Tsinghua University, Shenzhen 518055, PR China.
*E-mail addresses:* maoyu@hfut.edu.cn (Y. Mao), jiangyy@sz.tsinghua.edu.cn (Y. Jiang).

https://doi.org/10.1016/j.talanta.2019.01.038
Received 3 September 2018; Received in revised form 4 January 2019; Accepted 9 January 2019
Available online 11 January 2019
0039-9140/ 

(dsDNA), or DNA sequences in DNA-RNA hybrid duplexes, regardless of nucleotide sequence, and without cleaving ssDNA or ssRNA [33,34]. Moreover, DSN can discriminate imperfectly matched duplexes (even single-base mismatched) from perfectly matched duplexes [35]. Therefore, DSN could serve as an important, practical tool in the biological and biochemical sciences because of its unique capabilities, such as full-length cDNA library normalization [36,37], SNP recognition [32,38], quantification of telomeric overhang [39], and DSN-mediated isothermal signal amplification [40–43].

SYBR Gold Dye is a less-toxic, stable and commercial nucleic acid dye, which can be used to label dsDNA, ssDNA, and RNA [44,45]. In addition, SYBR Gold emits low fluorescence by itself but exhibits approximately 1000-fold fluorescence enhancement by combining with nucleic acids, making it suitable as a fluorescent probe for the detection of nucleic acids [46–48]. Herein, we describe our efforts toward developing a much simpler, more rapid and highly selective biosensor for the sensitive detection of c-miRNAs in an assay based on DSN-assisted target recycling coupled with RCA. This biosensor is cost-effective and features a lower detection limit (down to 0.3fM) and higher selectivity for target c-miRNA with single-base mismatch discrimination. An important practical application of the present strategy is the detection of microRNA-21 (miR-21). Above all, this biosensor works well in real biological samples, including cancer cells and human serums, which will offer tremendous opportunities for the early diagnosis of cancers in the clinical settings.

## 2. Materials and methods

### 2.1. The reagents and human serum specimens

Duplex-specific nuclease (DSN) was purchased from Evrogen (Moscow, Russia). SYBR™ Gold Dye (10,000× Concentrate in DMSO) was purchased from Life technologies ™ (Eugene, Oregon, USA). The miRCURY™ RNA Isolation Kit-Biofluids was purchased from EXIQON (Woburn, MA, USA). Other common regents can be referred to our previous research [27]. The oligonucleotides used in this study were synthesized by Sangon Biotech Co., Ltd. (Shanghai, China), and the human serum specimens were donated by Peking University Shenzhen Hospital (Shenzhen, China).

### 2.2. The cell culture and miRNAs isolation

The breast cancer cell lines MDA-MB-231 (highly metastatic) and T47D (lowly invasive) were grown in RPMI 1640 (1 × with L-glutamine) medium (Corning), which was supplemented with 10% fetal bovine serum (Merck). Cells were cultured at 37 °C in a thermostatic incubator, which contained 5% $CO_2$ and aseptic water. The detailed procedure of c-miRNA isolation from cells and human serum specimens is shown in Supplementary material.

### 2.3. The process of circulating miRNAs detection

The analysis of c-miRNAs was performed in RNases-free tubes. 5 nM HP, 20U RNases inhibitor, 1 ×DSN master buffer, 0.1U duplex-specific nuclease (DSN), and 2 μL of target miRNA of various concentrations were reacted at 55 °C for 30 min. Then, 100 mM NaCl was added into the above reaction mixture and incubated at 30 °C for 10 min to inactivate the DSN. Afterwards, 1 mM dNTPs, 5 nM circular probe, 1 × RCA buffer, and 5U phi29 DNA polymerase were added into the above reaction solution, then incubated at 30 °C for 90 min. Finally, 1 × SYBR Gold Dye was added into the amplification products for fluorescence measurements ($\lambda_{ex}$ = 485 nm, $\lambda_{em}$ = 500–700 nm), The detailed apparatus is described in Supplementary material.

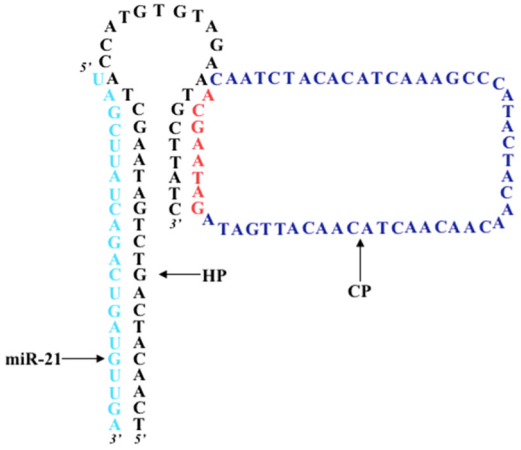


**Fig. 1.** The structures and interaction of the hairpin probe, the target c-miRNA and the circular probe.

## 3. Results and discussion

### 3.1. The design of the hairpin probe and circular probe

MiR-21 is an oncogenic c-miRNA that is overexpressed in many human cancers, making it an important biomarker for cancers screening and progression [49,50]. Thus, it was chosen as a model c-miRNA in this study. The biosensor mainly contains a label-free DNA hairpin probe (HP: 5′ -*TCAACATCAGTCTGATAAGCTA*CCATGTGTAGAA**TGCT TATC -3′**) and a DNA circular probe (CP: 5′-AGCACAATACACATCAA AGCCCATACTACAA- CAACTACAACATTGATAGAT-3′). The HP consists of two structure domains: the italicized bases are complementary to the target c-miRNA (miR-21: 5′-UAGCUUAUCAGA- CUGAUGUUGA-3′) to trigger the DSN reaction, and the bases in boldface serve as a primer of the CP to initialize the RCA reaction as shown in Fig. 1.

### 3.2. The mechanism of circulating miRNA assay

The principle of the new biosensor for the sensitive assay of c-miRNA is shown in Fig. 2. DSN recognizes the DNA-miRNA hybrid duplex that was formed through the hairpin probe (HP) hybridizing with the target c-miRNA and mediates the digestion of HP in the hybrid duplex. Upon digestion, the target c-miRNA is released and recycled for another round of hybridization and digestion. Therefore, in this practical protocol, DSN enables target recycling, and more importantly, the residual HP sequences can be further used as a primer of the CP to trigger the RCA reaction, which generates thousands of long ssDNA of

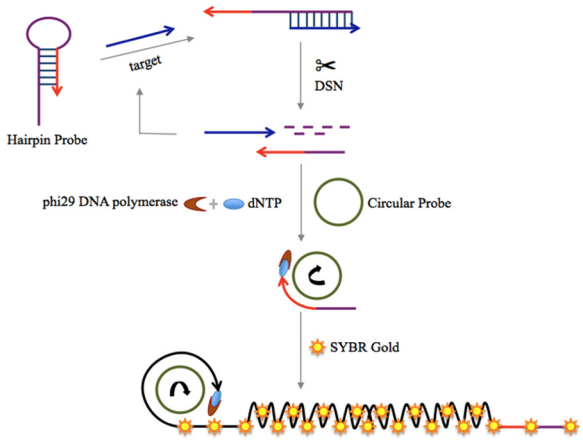


**Fig. 2.** Diagram of DSN-assisted target recycling coupled with rolling circle amplification strategy for the sensitive detection of circulating microRNAs.

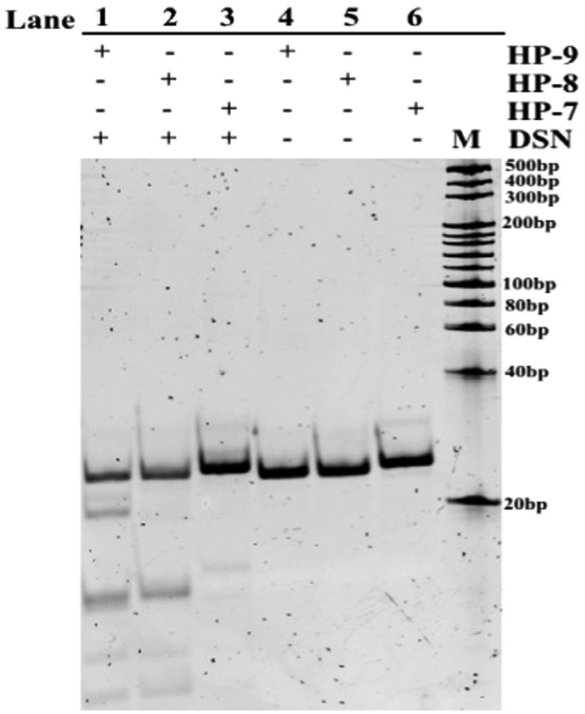


**Fig. 3.** A 20% native polyacrylamide gel electrophoresis (PAGE) for the optimization of hairpin probes. M is a DNA marker, Lane 1 HP-9 + DSN, Lane 2 HP-8 + DSN, Lane 3 HP-7 + DSN, Lane 4 HP-9, Lane 5 HP-8, Lane 6 HP-7, respectively. (HP-9, HP-8, and HP-7 refer to the number of base pairs in the stem structure).

various lengths. The products of RCA can be simply quantified by SYBR Gold dye. Conversely, in the absence of target c-miRNA in the detection system, the HP can coexist with DSN and maintain its stable hairpin configuration, providing a lower background fluorescence signal for the biosensor. This entire concept formed the basis for an extremely selective, sensitive, rapid and simple biosensor for the assay of c-miRNAs.

### 3.3. The optimization of hairpin probes

Since DSN cleaves dsDNA, if the length of the complementary region of the HP is too long, then the HP can be digested by DSN without the target c-miRNA, resulting in a false-positive signal. To make the biosensor more accurate, we optimized the stem length of the HP. As shown in Fig. 3, the length of 8 or 9 base pairs in the stem of the HPs (HP-8: 5′-TCAACATCAGTCTGATAAGCTACCATGTGTAGATAGCTTATC-3′, HP-9: 5′-TCAACATCAGTCTGATAAGCTACCATGTGTAGATAGCTTATC-3′) resulted in digestion by DSN. However, the 7-base-pair-stem length of the HP hairpin structure (HP: 5′-TCAACATCAGTCTGATAAGCTACCATGTGTAGAATGCTTATC-3′**)** remained stable. In HP-8, HP-9, and HP, the underlined bases indicate the sequences of the hairpin probe stems. These results indicate that when the length of double-stranded DNA is less than 8 base pairs, the structure is resistant to digestion by DSN. Therefore, we chose 7 base pairs as the stem length for the HP in this study.

### 3.4. The feasibility of the biosensor for circulating miRNA assay

We assessed the feasibility of DSN-assisted target recycling for RCA, as demonstrated in Fig. 4. We performed 20% native polyacrylamide gel electrophoresis to demonstrate DSN-assisted target recycling as shown in Fig. 4**A**, the detailed procedure is shown in Supplementary material. Lanes 1 and 2 show the primary position of miR-21 and HP, respectively. Lanes 3 and 4 indicate that there is no interaction when DSN is mixed with miR-21 or with HP. Lane 5 shows that target miR-21

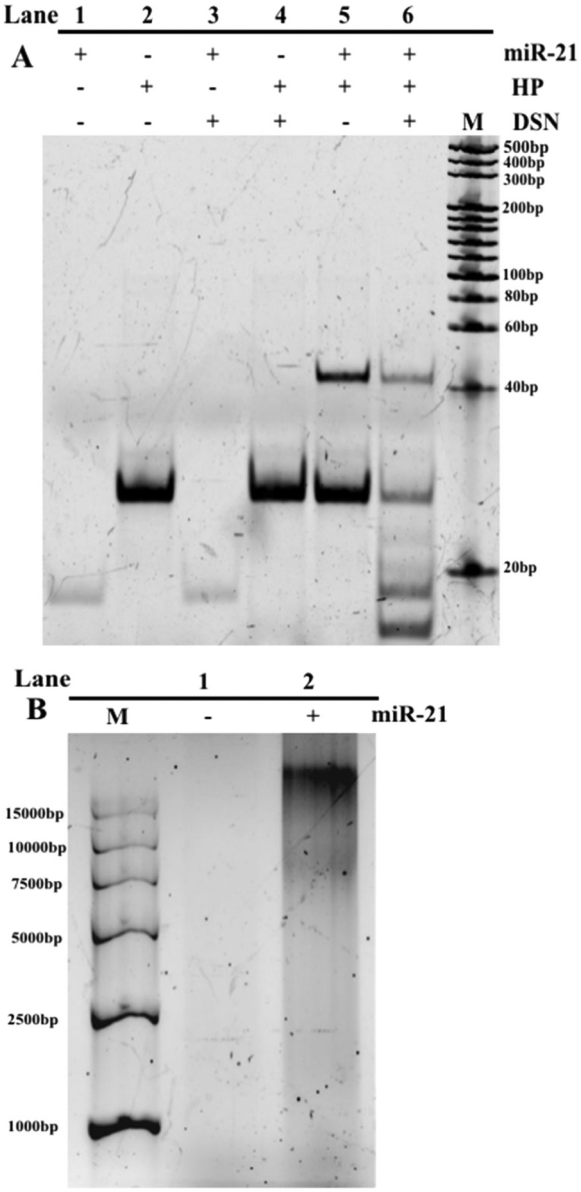


**Fig. 4.** A. 20% native PAGE for the assay of DSN-assisted target recycling. Lane 1 miR-21, Lane 2 HP, Lane 3 miR-21 + DSN, Lane 4 HP + DSN, Lane 5 miR-21 + HP, Lane 6 miR-21 + HP + DSN. B. 0.4% agarose gel electrophoresis for the evaluation of amplified products by DSN-assisted target recycling coupled with rolling circle amplification. Lane 1 and Lane 2 are amplified results without and with the miR-21, respectively.

can hybridize with HP to form miR-21-HP duplexes, which form a new clear band in the gel. Additionally, when the target miR-21, HP and DSN are all present in the detection system, a new clear band with a lower molecular weight than HP appears in the bottom of the Lane 6, while the band corresponding to the target miR-21 is still present, suggesting that DSN cleaves the DNA only in the miRNA-DNA duplexes, and the target c-miRNA is released and recycled for another reaction. These results indicate the effectiveness of DSN-assisted target recycling.

We verified the authenticity of the RCA reaction in the proposed biosensor with 0.4% agarose gel electrophoresis in Fig. 4**B**, the detailed procedure is shown in Supplementary material. Lane 1 shows that there are no products of RCA without the target miR-21. In contrast, in the presence of target miR-21, the RCA reaction is initiated to produce a larger number of ssDNA as shown in Lane 2. These results powerfully demonstrate the feasibility of DSN-assisted target recycling coupled with RCA for the detection of c-miRNAs.

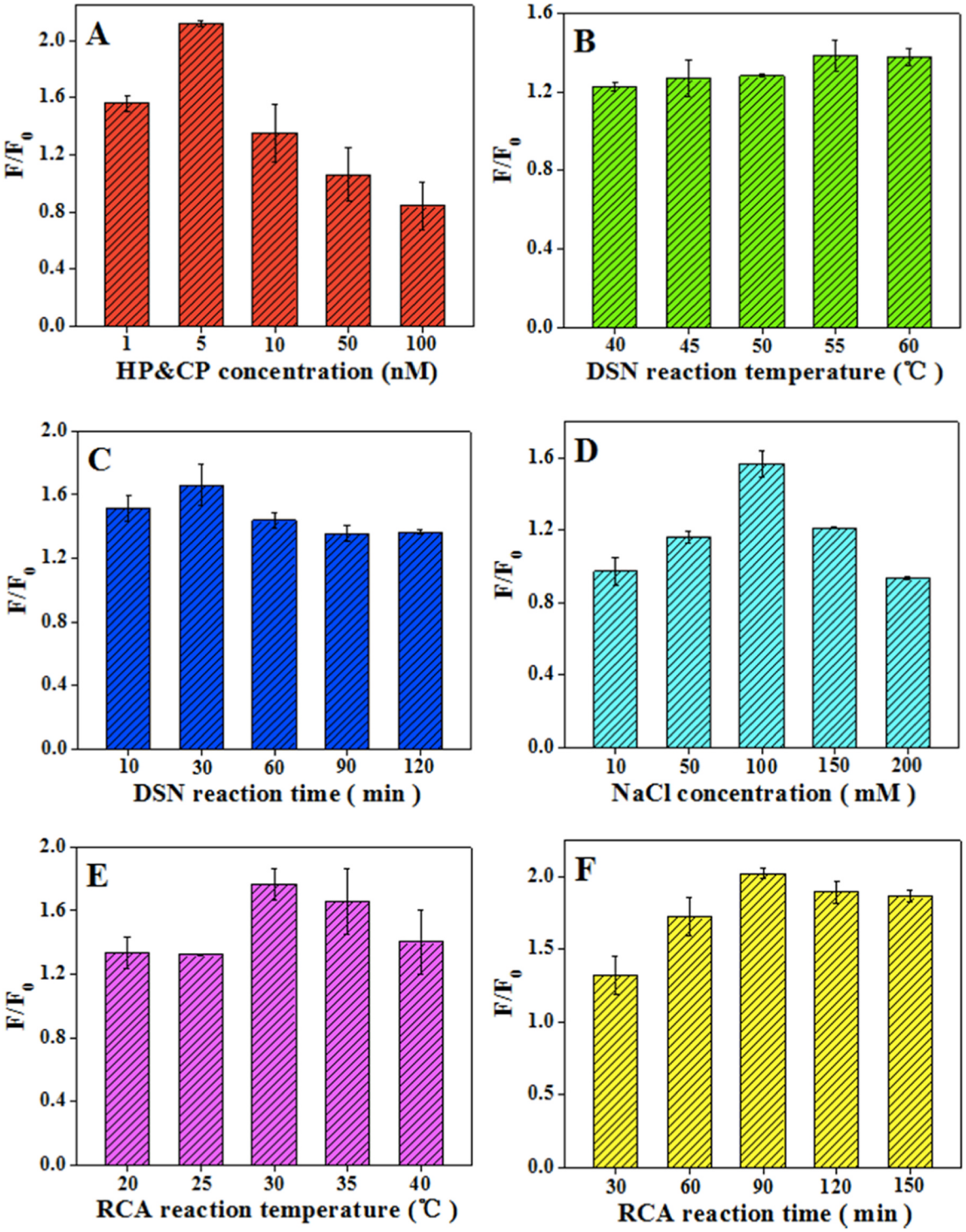


**Fig. 5.** A. The optimization of the concentrations of hairpin probe (HP) and circular probe (CP). B. The optimization of DSN incubation temperature. C. The optimization of DSN incubation time. D. The optimization of NaCl concentration. E. The optimization of RCA incubation temperature. F. The optimization of RCA incubation time. The error bars represent the standard deviations of three independent experiments.

### *3.5. The optimization of assay conditions*

To develop the best possible detection system, we optimized the concentrations of the HP and the CP, the DSN reaction temperature, the DSN reaction time, the concentration of NaCl, the RCA reaction temperature and the RCA reaction time. The experimental results are shown in Fig. 5, where F and $F_0$ are the fluorescence intensity ($\lambda_{ex}$ = 485 nm, $\lambda_{em}$ = 544 nm) with and without target c-miRNA, respectively. During optimization of the concentration (1–100 nM) of HP and CP (Fig. 5**A**), the highest value of $F/F_0$ was obtained when 5 nM of each HP and CP was used. Next, during the optimization of DSN reaction temperature (40–60 °C), the maximum $F/F_0$ value was achieved at 55 °C (Fig. 5**B**). In a similar fashion, we optimized the reaction time (10–120 min) of DSN (Fig. 5**C**) to 30 min. At the end of the DSN reaction, to avoid impacts on the RCA reaction, we added NaCl to inactivate the DSN. During the optimization of the NaCl concentration

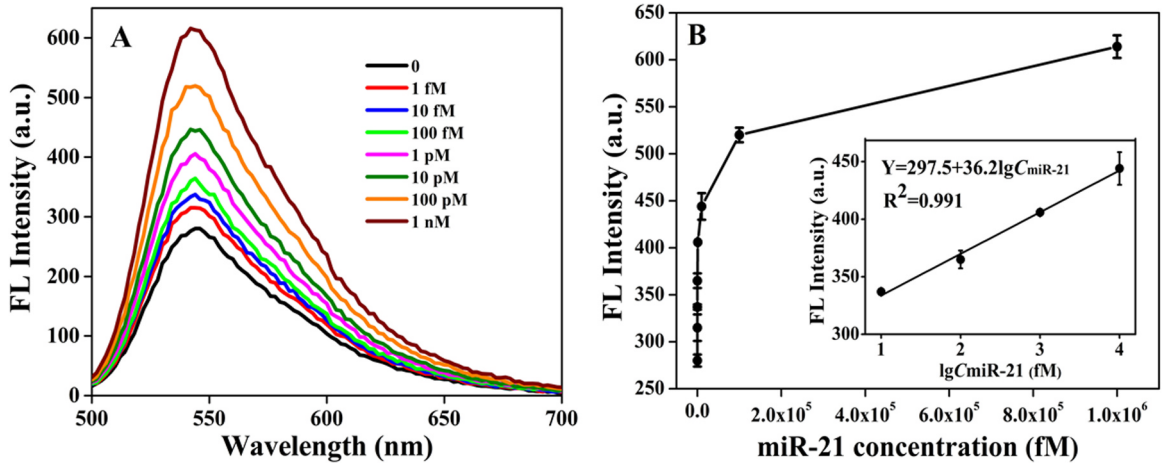


**Fig. 6.** A. The fluorescence intensity with different concentrations of miR-21 (0, 1 fM, 10 fM, 100 fM, 1 pM, 10 pM, 100 pM, 1 nM). B. The calibration curve between the fluorescence intensity and the logarithm of concentration of miR-21 (inset figure). The error bars show the standard deviation of three independent experiments.

(10–200 mM) (Fig. 5**D**), the maximum $F/F_0$ value was reached at 100 mM. Similarly, the RCA reaction temperature (20–40 °C) was optimized (Fig. 5**E**) at 30 °C. Finally, the RCA reaction time (30–150 min) was optimized (Fig. 5**F**) at 90 min. Therefore, the optimum conditions chosen for the following experiments were 5 nM HP, 5 nM CP, DSN reaction temperature of 55 °C, DSN reaction time of 30 min, 100 mM NaCl, RCA reaction temperature of 30 °C and RCA reaction time of 90 min.

### 3.6. The sensitivity of the circulating miRNA assay

To evaluate the performance of the biosensor for c-miRNAs detection, we found a non-linear fluorescence enhancement as the concentrations of miR-21 was increased from 0 to 1 nM as shown in Fig. 6**A**. However, the correlation between the fluorescence intensity (Y) and the logarithm of the concentration of the miR-21 ($lgC_{miR\text{-}21}$) was linear (Fig. 6**B**). The regression equation is $Y = 297.5 + 36.2\ lgC_{miR\text{-}21}$ with $R^2$ (correlation coefficient) = 0.991. According to the 3σ rule [51], the limit of detection was evaluated to be 0.3 fM, and the detection system has a wide linear dynamic range of four orders of magnitude.

### 3.7. The selectivity of the circulating miRNAs assay system

Most of the c-miRNAs share levels of homology c-miRNAs depending on their family, thus, it is very important to distinguish between homologous c-miRNAs that always have 1–3 base differences. We performed the selectivity experiments using perfectly matched miR-21, one-base-mispairing to miR-21 (M1: 5′-UAGCUUAUCAGAC**C**GAUGUUGA-3′), two-base-mispairing to miR-21 (M2: 5′-UAGC**A**UAUCAGAC**C**GAUGUUGA-3′), and three-base-mispairing to miR-21 (M3: 5′-UAGC**AA**AUCAGAC**C**GAUGUUGA-3′). In M1, M2, and M3, the bases in boldface are the mismatched sites compared with perfectly matched miR-21. The results in Fig. 7 show that compared with the perfectly matched miR-21, the values of $F\text{-}F_0$ for M1, M2 and M3 were only approximately 31.4%, 13.8%, and 10.1%, respectively. This result indicates that the biosensor has the ability to strongly distinguish between single-base mismatched c-miRNAs and perfectly matched c-miRNAs, suggesting a high specificity for the c-miRNA assay.

### 3.8. Application in complex biological samples

To verify the ability of the developed protocol to quantitatively assay c-miRNAs in real biological samples, we tested the proposed biosensor in human breast cancer cell lines MDA-MB-231 (highly metastatic) and T47D (lowly invasive) with total miRNAs as shown in Fig. 8. We also detected the miR-21 in total c-miRNAs that isolated from human serum specimens using the proposed biosensor as shown in Fig. 9. The results show that our biosensor could assay for c-miRNAs in cancer cells and human serums.

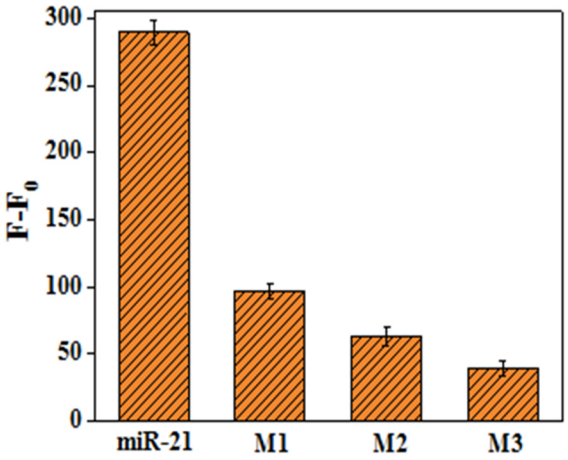


**Fig. 7.** The specificity of c-miRNA detection. The fluorescence intensity with different target miRNAs (miR-21, M1, M2, and M3).

We also evaluated the ability of the proposed biosensor to perform in the presence of interference by testing its performance in 10% human serums. Human serums injected with the miR-21 (1:1, V: V) at three different concentrations (10 pM, 50 pM and 100 pM) were tested. The results in Table 1 clearly show that the standard addition recovery rates of the proposed biosensor are from 117% to 122% in 10% human serums. This suggests that this biosensor has significant potential for the detection of c-miRNAs in complex biological samples.

## 4. Conclusions

In conclusion, a simple, rapid and highly sensitive biosensor has been developed to selectively detect c-miRNAs. Notably, the newly developed assay has obvious advantages in terms of simplicity, rapidity and cost-effectiveness, as well as a great capability to distinguish one-base mispairing c-miRNA and a higher sensitivity toward target c-miRNA with a much lower detection limit of 0.3 fM and a much wider linear dynamic range of four orders of magnitude. These characteristics make this method a valuable alternative to the previous approach as shown in Table S2. Finally, the proposed system performed well in real,

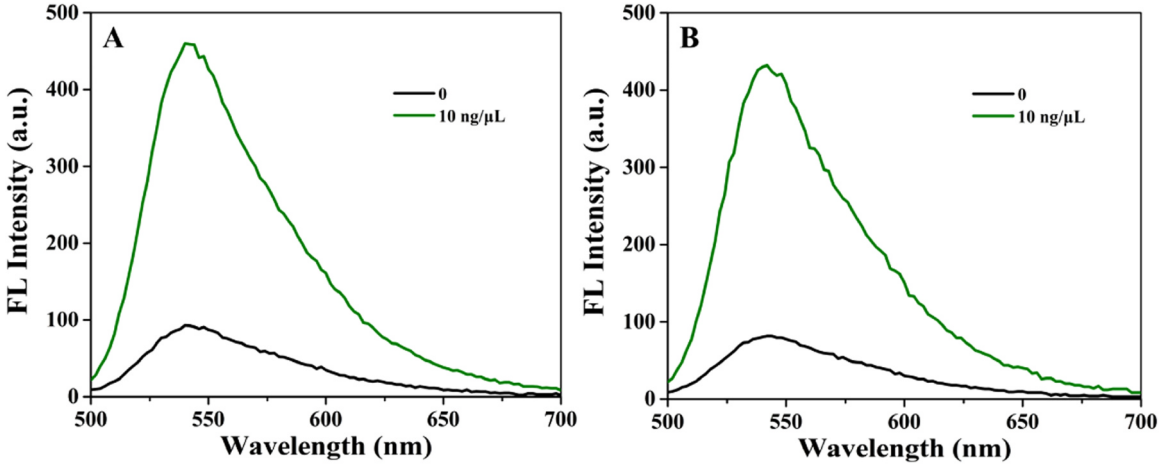


**Fig. 8.** A. The fluorescence intensity of miR-21 in 10 ng/μL total miRNAs that extracted from MDA-MB-231 highly metastatic breast cancer cell line. B. Fluorescence intensity of miR-21 in 10 ng/μL total miRNAs that extracted from T47D lowly invasive breast cancer cell line.

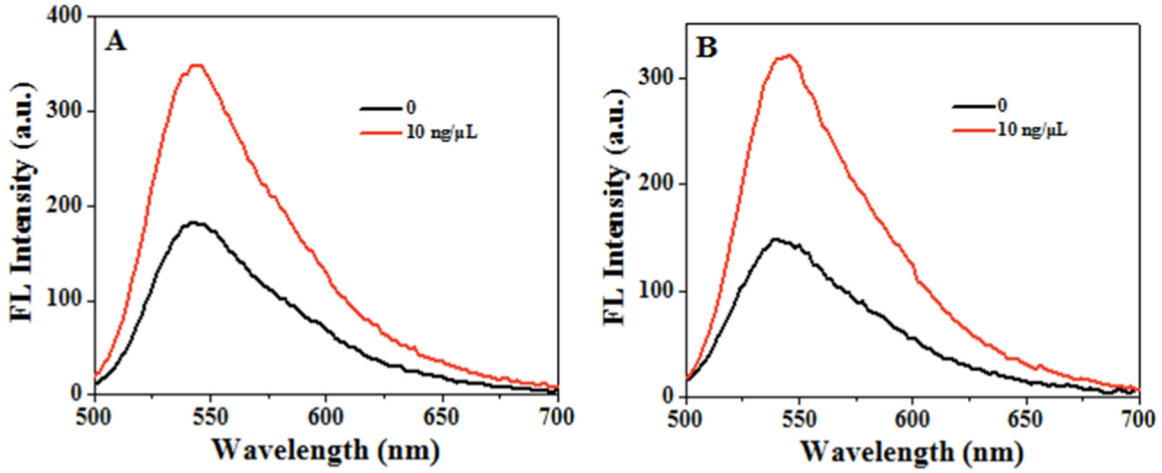


**Fig. 9.** A. The fluorescence intensity of c-miR-21 in 10 ng/μL total c-miRNAs that extracted from human serum specimen 1. B. The fluorescence intensity of c-miR-21 in 10 ng/μL total c-miRNAs that extracted from human serum specimen 2.

**Table 1**
The detection of miR-21 in 10% human serum specimens.

| | DSN assisted target recycling - RCA assay | | | |
|---|---|---|---|---|
| Sample | Added/(pM) | Mean found[a]/(pM) | Mean recovery[b]/(%) | RSD[c]/(%) |
| 1 | 10 | 12.25 | 122.57 | 4.29 |
| 2 | 50 | 56.41 | 112.83 | 2.26 |
| 3 | 100 | 117.23 | 117.23 | 0.88 |

[a] Mean concentration of three independent experiments.
[b] Mean recovery (%) = ($C_{\text{mean found}}/C_{\text{added}}$) × 100%.
[c] Relative standard deviation of three independent experiments.

complex biological samples. The utility of this protocol was illustrated by the detection of miR-21, and the approach may be expanded to detect other disease-related c-miRNAs, which offers a huge potential in miRNAs profile assay, miRNAs function research, biomedical research and for the early diagnosis of cancers based on miRNAs detection in the clinical settings.

## Acknowledgements

The National Natural Science Foundation of China, China (No. 21402105), and Shenzhen municipal government SZSITIC, China (CXB201104210013) supported this work.

## Appendix A. Supporting information

Supplementary data associated with this article can be found in the online version at doi:10.1016/j.talanta.2019.01.038

## References

[1] P.S. Mitchell, R.K. Parkin, E.M. Kroh, B.R. Fritz, S.K. Wyman, E.L. Pogosova-Agadjanyan, A. Peterson, J. Noteboom, K.C. O'Briant, A. Allen, D.W. Lin, N. Urban, C.W. Drescher, B.S. Knudsen, D.L. Stirewalt, R. Gentleman, R.L. Vessella, P.S. Nelson, D.B. Martin, M. Tewari, Circulating microRNAs as stable blood-based markers for cancer detection, Proc. Natl. Acad. Sci. USA 105 (2008) 10513–10518.
[2] P.Y. Lin, P.C. Yang, Circulating miRNA signature for early diagnosis of lung cancer, EMBO Mol. Med. 3 (2011) 436–437.
[3] M. Hanke, K. Hoefig, H. Merz, A.C. Feller, I. Kausch, D. Jocham, J.M. Warnecke, G. Sczakiel, A robust methodology to study urine microRNA as tumor marker: microRNA-126 and microRNA-182 are related to urinary bladder cancer, Urol. Oncol. 28 (2010) 655–661.
[4] N.J. Park, H. Zhou, D. Elashoff, B.S. Henson, D.A. Kastratovic, E. Abemayor, D.T. Wong, Salivary microRNA: discovery, characterization, and clinical utility for oral cancer detection, Clin. Cancer Res. 15 (2009) 5473–5477.
[5] D. Zubakov, A.W. Boersma, Y. Choi, P.F. van Kuijk, E.A. Wiemer, M. Kayser, MicroRNA markers for forensic body fluid identification obtained from microarray screening and quantitative RT-PCR confirmation, Int. J. Leg. Med. 124 (2010) 217–226.
[6] D.P. Bartel, MicroRNAs: genomics, biogenesis, mechanism, and function, Cell 116 (2004) 281–297.
[7] E. Huntzinger, E. Izaurralde, Gene silencing by microRNAs: contributions of translational repression and mRNA decay, Nat. Rev. Genet. 12 (2011) 99–110.
[8] M.S. Ebert, P.A. Sharp, Roles for microRNAs in conferring robustness to biological

processes, Cell 149 (2012) 515–524.
[9] J. Hayes, P.P. Peruzzi, S. Lawler, MicroRNAs in cancer: biomarkers, functions and therapy, Trends Mol. Med. 20 (2014) 460–469.
[10] D. Chen, C.P. Goswami, R.M. Burnett, M. Anjanappa, P. Bhat-Nakshatri, W. Muller, H. Nakshatri, Cancer affects microRNA expression, release, and function in cardiac and skeletal muscle, Cancer Res. 74 (2014) 4270–4281.
[11] E.N. Olson, MicroRNAs as therapeutic targets and biomarkers of cardiovascular disease, Sci. Transl. Med. 6 (2014) 239ps233.
[12] W. Wang, G. Sun, L. Zhang, L. Shi, Y. Zeng, Circulating microRNAs as novel potential biomarkers for early diagnosis of acute stroke in humans, J. Stroke Cerebrovasc. Dis. 23 (2014) 2607–2613.
[13] C. Roth, B. Rack, V. Muller, W. Janni, K. Pantel, H. Schwarzenbach, Circulating microRNAs as blood-based markers for patients with primary and metastatic breast cancer, Breast Cancer Res. 12 (2010) R90.
[14] H. Mlcochova, R. Hezova, M. Stanik, O. Slaby, Urine microRNAs as potential noninvasive biomarkers in urologic cancers, Urol. Oncol. 32 (41) (2014) e41–49.
[15] A. Valoczi, C. Hornyik, N. Varga, J. Burgyan, S. Kauppinen, Z. Havelda, Sensitive and specific detection of microRNAs by northern blot analysis using LNA-modified oligonucleotide probes, Nucleic Acids Res. 32 (2004) e175.
[16] H. Konishi, D. Ichikawa, S. Komatsu, A. Shiozaki, M. Tsujiura, H. Takeshita, R. Morimura, H. Nagata, T. Arita, T. Kawaguchi, S. Hirashima, H. Fujiwara, K. Okamoto, E. Otsuji, Detection of gastric cancer-associated microRNAs on microRNA microarray comparing pre- and post-operative plasma, Br. J. Cancer 106 (2012) 740–747.
[17] A. Gordanpour, R.K. Nam, L. Sugar, S. Bacopulos, A. Seth, MicroRNA detection in prostate tumors by quantitative real-time PCR (qPCR), J. Vis. Exp. (2012) e3874, https://doi.org/10.3791/3874.
[18] M. Labib, N. Khan, S.M. Ghobadloo, J. Cheng, J.P. Pezacki, M.V. Berezovski, Three-mode electrochemical sensing of ultralow microRNA levels, J. Am. Chem. Soc. 135 (2013) 3027–3038.
[19] W. Cai, S. Xie, Y. Tang, Y. Chai, R. Yuan, J. Zhang, A label-free electrochemical biosensor for microRNA detection based on catalytic hairpin assembly and in situ formation of molybdophosphate, Talanta 163 (2017) 65–71.
[20] Q. Wang, B.C. Yin, B.C. Ye, A novel polydopamine-based chemiluminescence resonance energy transfer method for microRNA detection coupling duplex-specific nuclease-aided target recycling strategy, Biosens. Bioelectron. 80 (2016) 366–372.
[21] Y. Xu, D. Li, W. Cheng, R. Hu, Y. Sang, Y. Yin, S. Ding, H. Ju, Chemiluminescence imaging for microRNA detection based on cascade exponential isothermal amplification machinery, Anal. Chim. Acta 936 (2016) 229–235.
[22] P. Bakthavathsalam, G. Longatte, S.O. Jensen, M. Manefield, J.J. Gooding, Locked nucleic acid molecular beacon for multiplex detection of loop mediated isothermal amplification, Sens. Actuators B: Chem. 268 (2018) 255–263.
[23] R. Deng, K. Zhang, J. Li, Isothermal Amplification for MicroRNA Detection: from the Test Tube to the Cell, Acc. Chem. Res. 50 (2017) 1059–1068.
[24] W. Nie, Q. Wang, X. Yang, H. Zhang, Z. Li, L. Gao, Y. Zheng, X. Liu, K. Wang, High sensitivity surface plasmon resonance biosensor for detection of microRNA based on gold nanoparticles-decorated molybdenum sulfide, Anal. Chim. Acta 993 (2017) 55–62.
[25] Q. Li, Q. Wang, X. Yang, K. Wang, H. Zhang, W. Nie, High sensitivity surface plasmon resonance biosensor for detection of microRNA and small molecule based on graphene oxide-gold nanoparticles composites, Talanta 174 (2017) 521–526.
[26] M. Liu, J.P. Song, S.M. Shuang, C. Dong, J.D. Brennan, Y.F. Li, A graphene-based biosensing platform based on the release of DNA probes and rolling circle amplification, ACS Nano 8 (2014) 5564–5573.
[27] T. Fan, Y. Mao, F. Liu, W. Zhang, J. Yin, Y. Jiang, Dual signal amplification strategy for specific detection of Circulating microRNAs based on Thioflavin T, Sens. Actuators B: Chem. 249 (2017) 1–7.
[28] H. Xu, S. Zhang, C. Ouyang, Z. Wang, D. Wu, Y. Liu, Y. Jiang, Z.-S. Wu, DNA nanostructures from palindromic rolling circle amplification for the fluorescent detection of cancer-related microRNAs, Talanta (2018), https://doi.org/10.1016/j.talanta.2018.07.090.
[29] G.D. Hamblin, K.M. Carneiro, J.F. Fakhoury, K.E. Bujold, H.F. Sleiman, Rolling circle amplification-templated DNA nanotubes show increased stability and cell penetration ability, J. Am. Chem. Soc. 134 (2012) 2888–2891.
[30] A. Fire, S.Q. Xu, Rolling Replication of Short DNA Circles, Proc. Natl. Acad. Sci. USA 92 (1995) 4641–4645.
[31] W. Zhao, M.M. Ali, M.A. Brook, Y. Li, Rolling circle amplification: applications in nanotechnology and biodetection with functional nucleic acids, Angew. Chem. Int. Ed. Engl. 47 (2008) 6330–6337.
[32] D.A. Shagin, D.V. Rebrikov, V.B. Kozhemyako, I.M. Altshuler, A.S. Shcheglov, P.A. Zhulidov, E.A. Bogdanova, D.B. Staroverov, V.A. Rasskazov, S. Lukyanov, A novel method for SNP detection using a new duplex-specific nuclease from crab hepatopancreas, Genome Res. 12 (2002).
[33] J. Zhang, D. Wu, Q. Chen, M. Chen, Y. Xia, S. Cai, X. Zhang, F. Wu, J. Chen, Label-free microRNA detection based on terbium and duplex-specific nuclease assisted target recycling, Analyst 140 (2015) 5082–5089.
[34] F. Ma, W.J. Liu, Q. Zhang, C.Y. Zhang, Sensitive detection of microRNAs by duplex specific nuclease-assisted target recycling and pyrene excimer switching, Chem. Commun. 53 (2017) 10596–10599.
[35] V.E. Anisimova, D.V. Rebrikov, D.A. Shagin, V.B. Kozhemyako, N.I. Menzorova, D.B. Staroverov, R. Ziganshin, L.L. Vagner, V.A. Rasskazov, S.A. Lukyanov, A.S. Shcheglov, Isolation, characterization and molecular cloning of duplex-specific nuclease from the hepatopancreas of the Kamchatka crab, BMC Biochem. 9 (2008) 14.
[36] P.A. Zhulidov, E.A. Bogdanova, A.S. Shcheglov, L.L. Vagner, G.L. Khaspekov, V.B. Kozhemyako, M.V. Matz, E. Meleshkevitch, L.L. Moroz, S.A. Lukyanov, D.A. Shagin, Simple cDNA normalization using kamchatka crab duplex-specific nuclease, Nucleic Acids Res. 32 (2004) e37.
[37] W.Z. Zhou, Y.M. Zhang, J.Y. Lu, J.F. Li, Construction and evaluation of normalized cDNA libraries enriched with full-length sequences for rapid discovery of new genes from Sisal (Agave sisalana Perr.) different developmental stages, Int. J. Mol. Sci. 13 (2012) 13150–13168.
[38] T. Muller, I. Ensminger, K.J. Schmid, A catalogue of putative unique transcripts from Douglas-fir (Pseudotsuga menziesii) based on 454 transcriptome sequencing of genetically diverse, drought stressed seedlings, BMC Genom. 13 (2012).
[39] Y. Zhao, H. Hoshiyama, J.W. Shay, W.E. Wright, Quantitative telomeric overhang determination using a double-strand specific nuclease, Nucleic Acids Res. 36 (2008) e14.
[40] Y. Zhang, W.J. Xu, Y.P. Zeng, C.Y. Zhang, Sensitive detection of DNA methyltransferase activity by transcription-mediated duplex-specific nuclease-assisted cyclic signal amplification, Chem. Commun. 51 (2015) 13968–13971.
[41] X.L. Huo, H. Yang, W. Zhao, J.J. Xu, H.Y. Chen, Nanopore-based electrochemiluminescence for detection of microRNAs via duplex-specific nuclease-assisted target recycling, ACS Appl. Mater. Interfaces 9 (2017) 33360–33367.
[42] K. Zhang, K. Wang, X. Zhu, F. Xu, M. Xie, Sensitive detection of microRNA in complex biological samples by using two stages DSN-assisted target recycling signal amplification method, Biosens. Bioelectron. 87 (2017) 358–364.
[43] X. Zhang, D. Wu, Z. Liu, S. Cai, Y. Zhao, M. Chen, Y. Xia, C. Li, J. Zhang, J. Chen, An ultrasensitive label-free electrochemical biosensor for microRNA-21 detection based on a 2'-O-methyl modified DNAzyme and duplex-specific nuclease assisted target recycling, Chem. Commun. 50 (2014) 12375–12377.
[44] R.S. Tuma, M.P. Beaudet, X.K. Jin, L.J. Jones, C.Y. Cheung, S. Yue, V.L. Singer, Characterization of SYBR gold nucleic acid gel stain: a dye optimized for use with 300-nm ultraviolet transilluminators, Anal. Biochem. 268 (1999) 278–288.
[45] Y. Xu, B. Jiang, J. Xie, Y. Xiang, R. Yuan, Y. Chai, Terminal protection of small molecule-linked ssDNA for label-free and sensitive fluorescent detection of folate receptor, Talanta 128 (2014) 237–241.
[46] D. Zheng, R. Zou, X. Lou, Label-free fluorescent detection of ions, proteins, and small molecules using structure-switching aptamers, SYBR Gold, and exonuclease I, Anal. Chem. 84 (2012) 3554–3560.
[47] Y. Mao, Y. Chen, S. Li, S. Lin, Y. Jiang, A graphene-based biosensing platform based on regulated release of an aptameric DNA biosensor, Sensors 15 (2015) 28244–28256.
[48] L. Lv, D. Li, R. Liu, C. Cui, Z. Guo, Label-free aptasensor for ochratoxin A detection using SYBR Gold as a probe, Sens. Actuators B: Chem. 246 (2017) 647–652.
[49] Y. Toiyama, M. Takahashi, K. Hur, T. Nagasaka, K. Tanaka, Y. Inoue, M. Kusunoki, C.R. Boland, A. Goel, Serum miR-21 as a diagnostic and prognostic biomarker in colorectal cancer, J. Natl. Cancer Inst. 105 (2013) 849–859.
[50] E. Larrea, C. Sole, L. Manterola, I. Goicoechea, M. Armesto, M. Arestin, M.M. Caffarel, A.M. Araujo, M. Araiz, M. Fernandez-Mercado, C.H. Lawrie, New concepts in cancer biomarkers: circulating miRNAs in liquid biopsies, Int. J. Mol. Sci. 17 (2016).
[51] J. Tang, D. Tang, J. Zhou, H. Yang, G. Chen, Nuclease cleavage-assisted target recycling for signal amplification of free-label impedimetric aptasensors, Chem. Commun. 48 (2012) 2627–2629.